Soil erosion assessment in a humid, Eastern Himalayan watershed undergoing rapid land use changes, using RUSLE, GIS and high-resolution satellite imagery

Nirmalya Chatterjee

Modeling Earth Systems and Environment

ISSN 2363-6203
Volume 6
Number 1

Model. Earth Syst. Environ. (2020)
6:533-543
DOI 10.1007/s40808-019-00700-0

Springer

Modeling Earth Systems and Environment (2020) 6:533–543
https://doi.org/10.1007/s40808-019-00700-0

ORIGINAL ARTICLE

Soil erosion assessment in a humid, Eastern Himalayan watershed undergoing rapid land use changes, using RUSLE, GIS and high-resolution satellite imagery

Nirmalya Chatterjee[1]

Received: 27 September 2019 / Accepted: 1 December 2019 / Published online: 9 December 2019

Abstract
The study aims to understand land degradation in the ≈ 2000 ha, humid and mountainous Papung khola catchment in the Sikkim Sivalik Range using the revised universal soil loss equation on a GIS platform. The catchment drains into the Tista River and is part of the data-sparse Eastern Himalayan ecoregion. Catchment land-use is changing from broadleaf forests to mixed land-use driven by rising population, and livelihood changes from primary production (forestry, agriculture) to service sectors (tourism, trade, construction). The study uses data on soil characteristics, ground and satellite precipitation and aerial land cover to predict potential soil erosion. Results indicate transitions in land cover/land use from forests to agriculture, disturbances due to construction and the potential increase in frequency of extreme climate events posing a unique risk to soils of the steep catchment causing decrease in soil cover and resultant loss of land productivity. The catchment can be currently categorized under a "very low" or "slightly erosive" regime (mean erosion rates 3.53 t ha^{-1} $year^{-1}$, with > 99% under cover of < 5 t ha^{-1} $year^{-1}$) with around three-quarters of the catchment under forest cover. High precipitation, intensification of diurnal and seasonal wetting-drying cycles, human disturbances to the top soil and rapid land use/land cover changes combining with the extreme topography and slow soil development is driving land degradation, which may stymie sustainable development and livelihood diversification in the future. Moderate erosion levels of ≈ 10 t ha^{-1} $year^{-1}$ can be expected in the future in areas with intact vegetation cover leading to complete top soil loss given the shallow profile depths.

Keywords Erosion prediction · RUSLE · Eastern Himalaya · Land degradation · Mountainous catchment

Abbreviations

RUSLE	Revised universal soil loss equation
GIS	Geographic information system

Introduction

Soils are the key substrate for the existence of the whole biosphere and form the key nutrient and mass exchange medium between the various components of the critical zone where most life exists: from the top of the bedrock to the canopy level. Soils are also the largest repositories of terrestrial carbon. The transport and cycling of water and carbon in our essentially carbon- and water-based life forms is through the soil.

Soil formation, *pedogenesis*, is a long-term natural process based on chemical and physical weathering of the earth's rocks taking hundreds to thousands of years for a few inches of soil. Erosion of soil, thus formed out of landscapes, is also a natural and inevitable process. However, when excessive soil erosion occurs, it affects the ability of the soil-scape to support a wide variety of plant and microbial species affecting biodiversity, and the soil's ability to act as a natural medium for exchange of water, organic carbon and mineral constituents–soil productivity is measured in this context.

Soil productivity is an indication of its ability to perform a wide gamut of ecosystem functions. While there is no universal soil productivity index, the quality of the soil can be described by how well a sample of soil responds to a set of standardized tests of its biological, chemical and physical properties, quantified by a set of indicators (Friedman et al. 2001).

✉ Nirmalya Chatterjee
c_nirmalya@wsu.edu

[1] Center for Biodiversity and Conservation, Ashoka Trust for Research in Ecology and the Environment, Eastern Himalaya–NE India Regional Office in Tadong, Gangtok, Sikkim, India

Soil erosion is quantified by the amount of soil lost as sediments from a given land surface with a developed soil profile. Soil erosion is a natural phenomenon and a continuation of the same geological process of weathering that give rise to soil formation from rock weathering. Soil profiles are additionally influenced by its interactions with the biological life that soils support—most notably the *biological indicators* of soil quality and its function as a repository of organic carbon. Soil erosion occurs due to both water and wind movement over the soil terrain, and due to its interactions with life forms.

Soil erosion is however very difficult to exactly quantify in the field due to extreme variations in rate and its close association with events, both natural (rainstorms, high winds) and human-induced (agricultural or construction activities). Lab- or field-based experiments under controlled conditions have, long been used as a proxy for real field based measurements with reasonable success to quantify erosion—especially in simpler topographies under agricultural land use (Wischmeier and Smith 1978). Erosive processes are however much more complicated and difficult to simulate in the lab when the target topography is complicated and has large variations in land use. In complex topographies the most common way of determining erosion has been computer modeling using empirical, and later physical process-based mathematical models (Morgan et al. 1998; Laflen et al. 1991, 1997, 1991; Nearing et al. 1990; Young et al. 1989; Morgan et al. 1984; Williams et al. 1983). These models' efficacy in predicting the quantity and spatial distribution of eroded sediments are dependent on the data available regarding the properties of the soil, the prevailing and historical weather patterns, the current land management practices and the general topographical parameters of the area. The simpler empirical models require lower number of parameters and usually at a lower spatial and temporal resolution. Empirical models are also computationally less intensive. The process based models allow more detailed modeling of the spatio-temporal distribution of erosion, but at the cost of more intense data collection effort and computation power.

Site location

The Tista River, along with its major tributary, the Rangit River form the Tista Basin, which is 55% coterminous with Sikkim state in North-Eastern India. The basin has one of the largest topographic, biological and climatic diversity in the world (India Meteorological Department 2015; Maharana et al. 2000; Rai and Sundriyal 1997; Rai et al. 1994). Sikkim has an elevation range between ≈ 200 and > 8500 m (Directorate of Census Operations 2012), is a biodiversity hotspot (Myers 1990; Marchese 2015) and has meteorological extremes with humid subtropical weather in the south and alpine, cold semi-desert in the far north. Temperatures in Sikkim range between > 35 °C close to the plains in summer, and < − 40 °C in the snow-bound mountains in the winter (India Meteorological Department 2015). Rainfall ranges between < 200 mm year^{-1} in the northern trans-Himalayan deserts to > 4000 mm year^{-1} in the southern sub-tropical forested uplands (India Meteorological Department 2015; Kumar and Krishnaswamy 2016).

In the current study, there are significant obstacles to using even soil erosion models to estimate erosion. The main obstacles are the lack of availability of data, complex nature of the topography and difficult logistics in collecting ground survey data and lack of continuity in available data sets. The micro-watershed that was chosen is in the Lesser Himalaya of Sikkim state. This effort was aimed to address the basic knowledge gap in modeling soil erosion processes in the Eastern Himalaya at small catchment scales, by creating a base-line prediction. The prediction relies on currently available survey topo-sheet and satellite elevation model data and ground station and gridded, satellite weather data and combines it with ground surveys to create an erosion assessment map of a micro-catchment with multiple land uses which is undergoing significant changes driven by population and livelihood changes.

The target catchment, the Papung *khola* watershed has an area of ≈ 20 km^2 (1989 ha) and empties directly into the Tista River, 5.7 km upstream of town of Singtam (East Sikkim district). The catchment is bound (clock-wise from the NE/E) by the Tista River, the Kalej *khola* catchment, the Kali *khola*–Kinchhu *khola* catchment and the Ben *khola* catchment. Both the Ben and Kalej *khola* also drain directly into the Tista as well, while the Kali/Kinchhu *khola* drain into the Rangit River to the west. The climate of the southern districts of Sikkim state come under the subtropical highland climate (Cwb) regime in the Köppen–Geiger Climate Classification system (Beck et al. 2018).

A map of the general vicinity of the Papung *khola* watershed with contour lines and local landmarks is given in Fig. 1. A notable importance of the Papung *khola* watershed is its location just upstream of the Tista Low-dam Power Project's 50-m-high Stage 5 dam (TLDP-V)—with the stream draining into the Tista River 3.7 river-kilometers upstream of the dam. Details of the E/NE draining catchments emptying into the Tista River are given in Table 1. Prior to setting up of long term monitoring of the Papung *khola* sub-watershed, a basic empirical soil erosion model is being applied for base line estimation of soil erosion.

Table 1 Details of the Papung *khola* and adjacent sub-watersheds

Stream (*khola*)	Stream length (km)	Average slope (%)	Elevation range (m)	Total area (ha)	Area under tea (ha)
Ben	6.75	25.6	2403–361	1677	19.39
Papung	6.85	22.9	2643–337	1989	149.83
Kalej	8.89	17.1	2639–274	3356	–

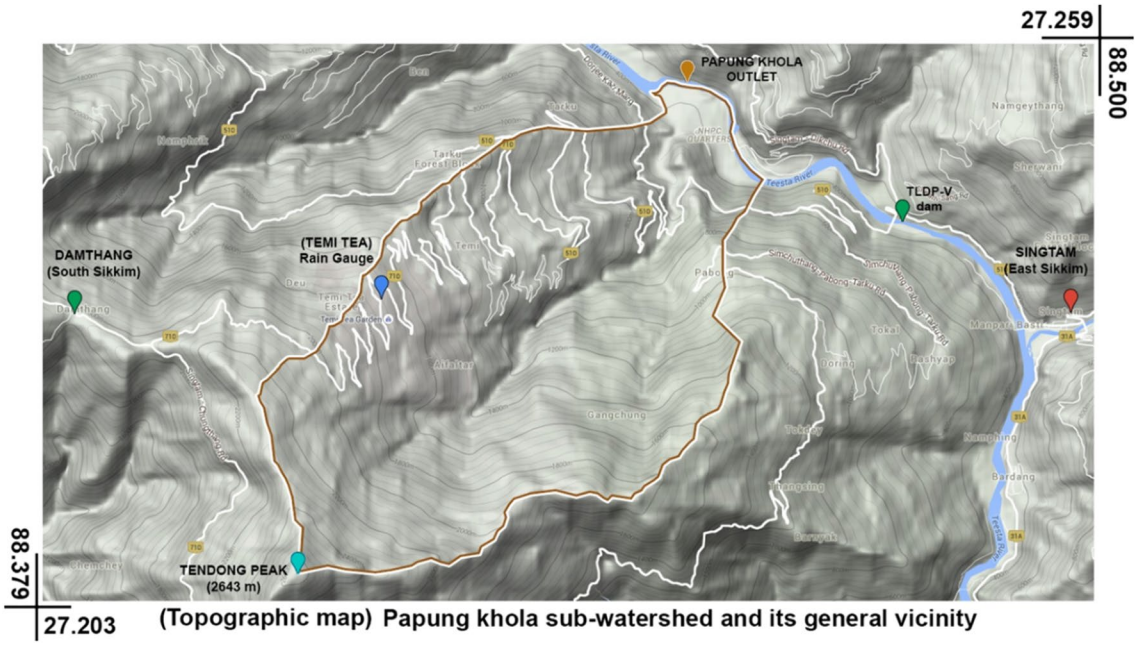

Fig. 1 Location map of the Papung *khola* watershed (white-brown outline) with local landmarks and topographical details

Methods

Thematic layer creation

Topography layer

The topography of the Papung *khola* sub-watershed was obtained from a combination of satellite digital elevation models (DEM) from the CartoSat 1 (ISRO India, 2014, 30 m) and ASTER Global DEM Version 2 (NASA USA and METI Japan, 2011, 30 m) data sets. The CartoSat DEM obtained was calibrated with a 1:50,000 ground survey toposheet of the Survey of India (Toposheet No. 78-A/8, 1963) and then verified with 47 ground survey points of topographical features and landmarks using a hand-held GPS (Garmin 62s) to account for satellite DEM errors and terrain changes since the ground-survey of 1963. The handheld GPS gave us an indication that validation was not manifestly erroneous. The use of two different DEM sources was necessitated by some pixels being improperly validated in shadow areas due to the complex topography. The CartoSat base DEM was corrected in these erroneous pixels with the more extensively validated ASTER dataset. Topographic continuity and polygon preparation issues were fixed using local extrapolation and grid-resampling on the GIS platform using data from the ASTER GDEM version 2. The corrected DEM was processed in ArcGIS 10.5 to obtain slope, flow accumulation and stream flow channels using the Spatial Analyst Toolbox. The lower-order stream channels were verified by ground survey of actual stream locations during the high runoff season (June-September). The final ground-calibrated DEM (30 m resolution) and validated stream flow map of the micro-watershed are shown in Fig. 2a.

Soil characteristics layer

The basic soil characteristics are obtained from random soil sampling within the watershed for determining soil texture, moisture content, and organic matter (OM) content. The National Bureau of Soil Survey data (NBSSLU&P,

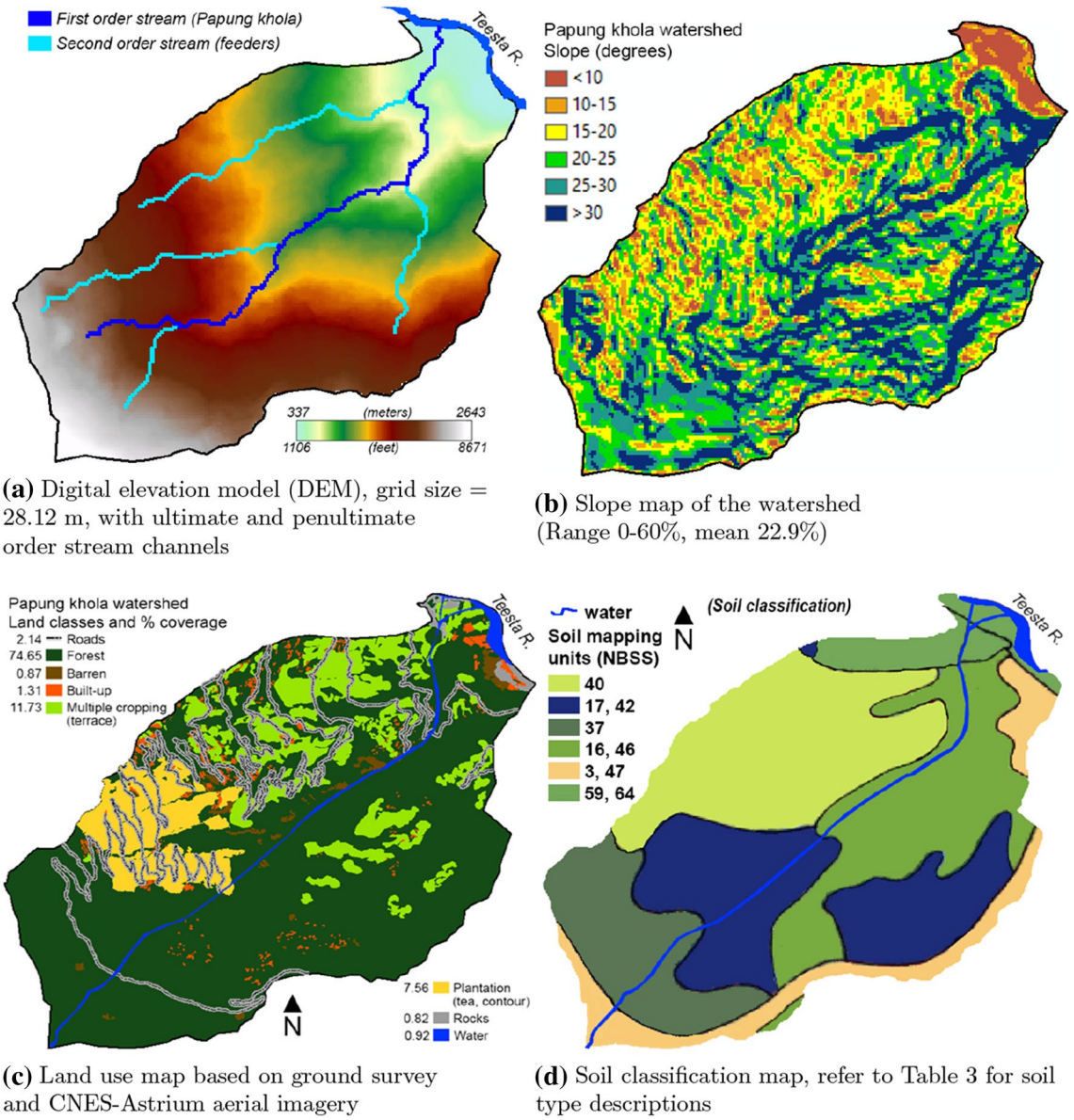

(a) Digital elevation model (DEM), grid size = 28.12 m, with ultimate and penultimate order stream channels

(b) Slope map of the watershed (Range 0-60%, mean 22.9%)

(c) Land use map based on ground survey and CNES-Astrium aerial imagery

(d) Soil classification map, refer to Table 3 for soil type descriptions

Fig. 2 Papung *khola* watershed terrain (elevation and slope), land use, and soil maps based on aerial and satellite imagery, and surveyed ground data

Nagpur, India) has published soil maps of Sikkim and lists the general properties of soils obtained from soil classification (Das et al. 2003, 2014). While the soil classification and data obtained from the NBSSLU&P soil maps were of insufficient resolution for our use case, the general soil distribution maps available were helpful in understanding the soil classification (soil series, map units and taxonomy). The details of the soil analysis from the samples collected within the watershed (texture, organic matter content, moisture content) are given for each land use class in Table 5. The total sample size of 60 were distributed over the four open-soil land-use classes (forest, multiple crop agriculture, plantation agriculture and barren), the built-up areas under houses and roads and areas under rock and rocky debris were not sampled for soil. Soils were sampled using a (2 cm int. dia.) corer till a depth of 50 cm.

Land use-land cover (LULC) layer using aerial imagery

The LULC regimes in place were manually checked along multiple elevational transects during ground survey after visual inspection of aerial maps obtained from CNES/Astrium aerial imagery. The LULC were classified into 8 different classes as shown in Table 2. The watershed area map was then color coded to create a LULC map as shown in Fig. 2c.

Table 2 Land-use class distribution in the Papung *khola* watershed

Land-use	Area (ha)	Area (%)	Description
Built-up	26	1.31	Residential, commercial and administrative buildings, other infrastructure
Plantation	150	7.54	Temi Tea Estate (88.54% of 169.16 ha total under tea, remaining areas are within the Ben *khola* watershed)
Multi-crop	233	11.71	Rotation cropping and seasonal fallow on terraces
Water	18	0.90	Streams, rivers, lakes
Forest	1485	74.66	Native dense forest and mixed tree/scrub patches
Rocks	16	0.81	Debris from rock slides and falls and land slips, gullies, ravines, pebble beds.
Roads	44	2.21	Roads and road-sides
Barren	17	0.86	Soil with no covering vegetation, road cuts
Total	1989	100	–

Erosion modeling

The quantification of soil lost in erosion can be modeled both using a process based model or an empirical mathematical model. Empirical models offer results with relatively little raw field collected data inputs, while process based models require a larger number of parameters as well as field measurements at higher spatio-temporal resolutions. Empirical models thus have an advantage for use in remote and relatively data sparse locations. The revised universal soil loss equation (RUSLE) (Wischmeier and Smith 1978; Renard et al. 1997) is used to quantify soil erosion in the watershed. RUSLE model typically does not offer any spatial sediment redistribution (sediment routing and deposition) in its results, however when combined with a cell or grid based digital elevation model within a geographical information system (GIS) environment, it can be suitably used to understand potential sediment movement in the form of erosion at the pixel level (in this case 900 m^2) in a watershed. The model calculates the average annual soil loss as:

$$A = R \times K \times LS \times C \times P \tag{1}$$

where A average annual soil loss in t ha^{-1} $year^{-1}$, R annual rainfall-runoff erosivity factor in 10^6 J mm ha^{-1} h^{-1} $year^{-1}$, K soil erodibility factor in t h $(10^6 \text{ J})^{-1}$ mm^{-1}, L slope length factor (dimensionless), S slope steepness factor (dimensionless), C cover and management factor (dimensionless), P conservation support practice factor (dimensionless).

Determination of RUSLE sub-factors

The 6 sub-factors in Eq. 1 above are input into the model as raster data layers. The value of the sub-factors for each cell in the DEM are assigned in the raster, these values can also be assigned region wise for a larger number of cells based on collected field data and available soil survey data. Rainfall, which affects water erosion rates, is itself significantly affected by the elevation and micro-topography at the point of measurement. While there are no universally acceptable models for spatial correlating of rainfall with topography and elevation from a single or a set of data points, we attempt to use the elevation data from the DEM in combination with gridded, satellite, precipitation data sets, with calibration using ground-based station data within the catchment.

In case there are multiple rainfall measurement points within or near a watershed, generation of interpolated rainfall values is done using the elevation data by kriging (or co-kriging), weighted linear interpolation, or Thiessen polygons (Berndt and Haberlandt 2018; Somodi et al. 2017; Samanta et al. 2012). These are widely used methods and give geo-statistically acceptable results. A wide variety of gridded precipitation data-sets are available (Matsuura and Willmott 2018; Fick and Hijmans 2017; Compo et al. 2011). The WorldClim v2.0 long-term, monthly gridded precipitation dataset was used because of availability at 1 km^2 grid resolution, keeping in mind the small size of the the target catchment.

The ground station (manual rain gauge at the Temi Tea Factory, elevation 1721 m) readings are representative of the mid-elevation of the Papung watershed (mean ± s.d. = 1400 ± 520 m). Daily rainfall data from the rain gauge is available for more than 20 years, which were used to calculate the long-term, monthly totals, and used to calibrate the WorldClim 2.0 dataset to obtain a reasonable variation of precipitation over the whole catchment for use in rainfall erosivity (R) sub-factor calculation (Arnoldus et al. 1980) as below:

$$R = \sum_{i=1}^{12} 1.735 \times 10^{\left(1.5 \log_{10}\left(\frac{p_i^2}{P}\right) - 0.08188\right)} \tag{2}$$

where P_i average monthly rainfall (mm), P average annual rainfall (mm).

Soil erodibility factor, K [t ha h ha^{-1} (10^6 J)$^{-1}$ mm^{-1}], is calculated from typical values for different land use classes (Table 3, Fig. 2d), and the soil texture and organic matter content measurements (Table 4) (Ismail and Ravichandran 2008). The soil profile infiltration data was gathered using a Decagon Devices Model S Mini-Disk infiltrometer. The detailed equations and methods to measure soil parameters and calculate the sub-factors are followed from the work of Ismail and Ravichandran (2008); and used as is. The relationship between the soil erodibility sub-factors is:

$$K = \frac{1}{100}\left(k_t \cdot k_o + k_s + k_p\right) \tag{3}$$

where k_t soil texture sub-factor, k_o soil organic matter sub-factor, k_s soil structure sub-factor, k_p soil profile permeability sub-factor.

The L and S (slope length and steepness) factors are generated as a data layer directly from the DEM, at an appropriate resolution using the topographical slope, hydrological flow direction and accumulation to calculate the LS (RUSLE topographical factor) for the model. The calculation method utilizes the Unit Stream Power Erosion and Deposition (USPED) model (Mitasova et al. 1996; Moore et al. 1993; Moore and Wilson 1992; Moore and Burch 1986; Rose et al. 1983). The LS data layer are directly generated as a raster product of the L and S individual data sets.

The L and S sub-factors are given by Oliveira et al. (2013), Mitasova et al. (1996):

$$L = (m+1)\left(\frac{\lambda_A}{22.1}\right)^m \tag{4}$$

where L the slope length factor at a point in the landscape, λ_A area of upland flow at the point, m an adjustable value

Table 3 Soil classification details of Papung *khola* watershed (per Das et al. 2003)

Map unit	Texture	Taxonomic sub-groups	Area (ha)	% of total
3	Major: Fine loam	Inceptisol (Pachic Haplumbrepts)	146.37	7.36
	Minor: Course loam	Inceptisol (Entic Haplumprebts)		
16	Major: Coarse loam	Entisol (Typic Udorthents)	3.83	0.19
	Minor: Coarse loam	Inceptisol (Lithic Haplumbrepts)		
17	Fine loam	Inceptisol (Ustric Dystrochrepts)	2.12	0.11
37	Major: Fine loam	Mollisol (Typic Paleudolls)	262.82	13.21
	Minor: Fine gravelly loam	Mollisol (Typic Hapludols)		
40	Major: Coarse loam	Inceptisol (Cumulic Haplumbrepts)	500.22	25.15
	Minor: Fine loam	Inceptisol (Typic Haplumbrepts)		
42	Major: Skeletal gravelly loam	Inceptisol (Umbric Dystrochrepts)	490.55	24.66
	Minor: Skeletal gravelly loam	Inceptisol (Typic Dystrochrepts)		
46	Major: Fine loam	Mollisol (Typic Argiudolls)	403.28	20.28
	Minor: Fine gravelly loam	Mollisol (Cumulic Hapludolls)		
47	Major: Coarse gravelly loam	Inceptisol (Pachic Haplumbrepts)	42.91	2.16
	Minor: Fine loam	Inceptisol (Umbric Dystrochrepts		
59	Major: Coarse loam	Mollisol (Cumulic Hapludolls)	79.09	3.98
	Minor: Fine gravelly loam	Mollisol (Typic Argiudolls)		
64	Major: Gravelly loam	Mollisol (Cumulic Hapludolls)	26.96	1.36
	Minor: Coarse loam	Entisol (Typic Udorthents)		
Total			1989	100

Table 4 Soil sample analysis results for samples from Papung *khola* watershed

Land-use class	Sample size (n)	Texture				Organic matter (% w/w)	Moisture (% w/w)
		Sand (%)	Silt (%)	Clay (%)	Textural class		
Forest	46	27	57	16	Fine silty loam	5.53	29
Multi-crop	7	51	32	17	Coarse medium loam	2.17	22
Plantation	5	49	17	34	Fine sandy clay loam	5.08	28
Barren	2	62	22	16	Fine sandy loam	1.47	22
Total	60						

depending on the soil's susceptibility to erosion, 22.1 constant to convert the actual plot length into number of unit plot lengths.

$$S = \left(\frac{\sin\left(\frac{\pi}{180} \times \theta_{\text{deg}}\right)}{0.09} \right)^{n} \tag{5}$$

where S slope steepness factor at a point in the landscape, θ_{deg} slope in degrees (multiplied by $\pi/180$ to convert to radians), n adjustable value dependent on the soil's susceptibility to erosion 0.09 slope gradient constant.

The equation governing the relation between the relation between flow accumulations and topographical slope (for every cell in the *LS* data raster) to the RUSLE *LS* sub-factor (the USPED model) is given by:

$$LS = 1.4 \times \left(F_A \times \frac{R_{\text{CS}}}{22.1} \right)^{m} \times \left(\frac{\sin\left(\frac{\pi}{180} \times \theta_{\text{deg}}\right)}{0.09} \right)^{n} \tag{6}$$

where F_A flow accumulation at a point on the landscape, R_{CS}] Raster cell size, θ_{deg}] slope in radians (multiply degree values by $\pi/180$), m, n adjustable value dependent on the soil's susceptibility to erosion, 0.09 slope gradient constant.

Cover management (*C*) and conservation support practice (*P*) factors are applied in a manner similar to the *K* factor, by taking values from the published literature (Das et al. 2003, 2014) and using the ground survey data of land use delineation as depicted in the land use map (Fig. 2c). The separate *C*-factor and *P*-factor data layers were attached as before in the GIS profile of the watershed.

GIS data layer generation

R, Annual rainfall-runoff erosivity factor The calculated *R* factor for the Papung *khola* watershed ranged from 3204 to 6786 (in MJ mm ha^{-1} h^{-1} year^{-1}). The rainfall pattern (20-year monthly averages) at the Temi Tea Estate rain gauge is shown in Fig. 3a. An *R*-factor calculated from a single rain gauge would ignore the change in rainfall with elevation, to correct this, an *R*-factor raster layer was prepared from a rainfall raster layer. The rainfall raster layer (Fig. 3b) was prepared from the DEM elevation data and rainfall variation over the catchment obtained from WorldClim 2.0 data (Fick and Hijmans 2017) after normalizing the latter with collected annual rain gauge data. This rainfall raster layer was used for getting the monthly rainfall at each pixel to calculate the *R*-factor raster layer (Fig. 3c).

K, Soil erodibility factor The calculated erodibility factors for the four different erodible land use classes are given in Table 5. The *K* values were assigned to every cell based on its land use classification, and four separate raster were generated based on the erodible land use classes above. A complete *K*-raster was generated using the raster mosaic function in ArcMap, the map is shown in Fig. 4a.

L, Slope length and S, Slope steepness factors (LS factor) *L*, Slope length and *S*, Slope steepness factors (*LS* factor). Slope map of the Papung *khola* watershed as obtained from the digital elevation map (Fig. 2a) is shown in Fig. 2b. The combined *LS* factor map is given in Fig. 4b.

C, Cover and management factor The *C*-factor of the different land use classes (Das et al. 2003, 2014) that are pertinent to the Papung *khola* watershed are given in Table 6, and a map is given in Fig. 4c.

P, Conservation support practice factor Since the forested and barren areas in watershed do not have any soil conservation practices in place the *P*-factor was assumed to be 1. The multiple cropping agriculture is done on terraces ($P = 0.1$) and the tea plantation have been planted with contour bunding ($P = 0.2$) (Das et al. 2003, 2014). The appropriate *P* values were applied for each cell for its land use class and the separate rasters mosaicked in ArcMap, the factors used are listed in Table 6. Spatial distribution of conservation support practice factor is given in Fig. 4d.

Results

The modeling results show that the watershed in its entirety is under an erosive regime categorized as "very low" or "slightly eroding" for Indian conditions (Dabral et al. 2008; Ismail and Ravichandran 2008; Bhattacharyya et al. 2015), with an average, watershed-wide, erosion rate of 3.4 t ha^{-1} year^{-1}. The erosion map of the watershed based on the modeling results are shown in Fig. 5. The lowest erosion sub-class (< 0.5 t ha^{-1} year^{-1}) covers ≈ 77% of the watershed, and 82% of the land is under permanent vegetation (forest or plantation) cover. Table 7 shows the erosion class (and sub-classes within the lowest eroding class) coverage in the catchment as predicted in this analysis.

Discussion

The watershed shows a huge potential of contributing sediments directly into the Tista River with rapid land use/land cover changes. The general steepness of the terrain and heavy precipitation regime and the poorly developed soils in this watershed suggest a heavy to extremely heavy chance of soil loss (Wischmeier and Smith 1978). The mitigating factor is the extensive ground cover in the watershed, with almost three quarters of under permanent, medium-to-dense forest cover, and around 8% under permanent plantation cover.

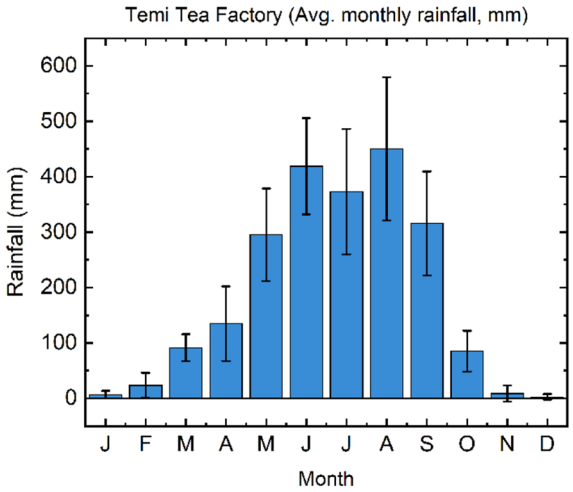

(a) Average, monthly rainfall between 1993–2013 (in mm) at the Temi Tea Factory rain-gauge (elev. 1721 m)

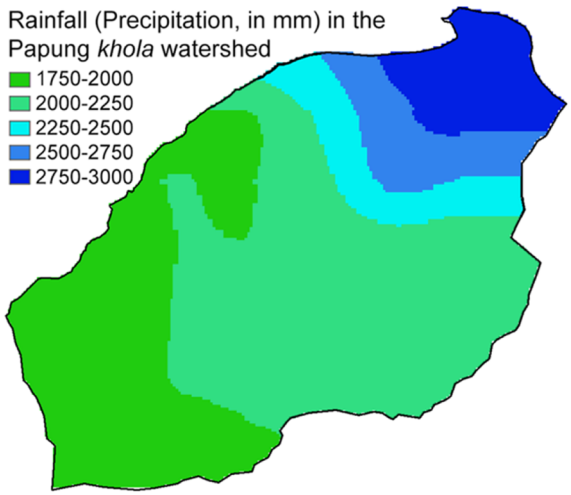

(b) Extrapolated rainfall (precipitation) map (Range 1754–2904 mm, mean 2146 mm)

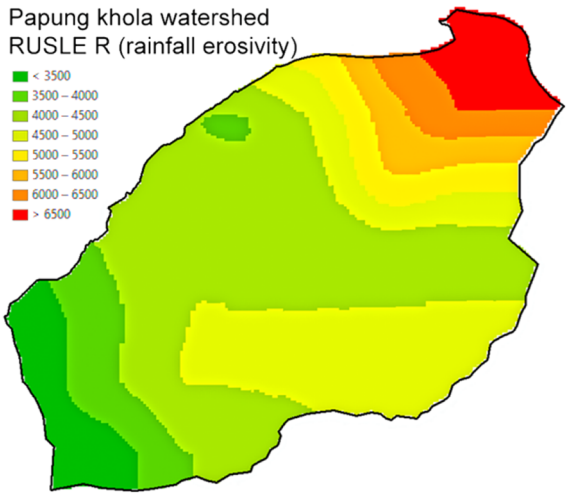

(c) Rainfall erosivity (R) factor map (Range: 3204–6786, mean 4572)

Fig. 3 Average monthly rainfall at Temi Tea Factory, and rainfall and rainfall erosivity (*R*) maps of the Papung *khola* watershed

Land-use classes lacking vegetation cover either permanently or seasonally (classes: barren, roads, multiple cropping agricultural terraces), are the biggest contributors to the soil loss from the watershed. The average *P*-factor in the watershed is very high at ≈ 0.8, indicating that conservation and support practices need to be put in place for mitigating soil loss. Since most of the watershed is under forest cover, the non-forest area will need to be closely monitored and managed to prevent soil loss and sediment efflux from the watershed. This will be both helpful in improving the soil within the watershed and also improve stream water quality inside and outside the watershed. Conservation methods like maintaining ground cover in agricultural areas, vegetating barren soils, and proper maintenance of existing terraces construction is important to prevent soil loss. Creation of contour bunding and check dams, will be necessary to trap sediments and lower the erosion due to runoff.

A comparison of the land use/cover classes and terrain slope in Fig. 2b, c with the predicted erosion map show that the soils in the forested tracts are under a higher erosive class, than those areas under permanent plantation or long-term multi-crop on account of the steeper slopes, the forested tracts are thus more vulnerable to erosion. Such conditions as in the steep, forested slopes thus have greater chances to contribute to soil loss in case of forest diversion to alternative land uses. Thus, monitoring of land use changes, and implementation of zoning and land use policies

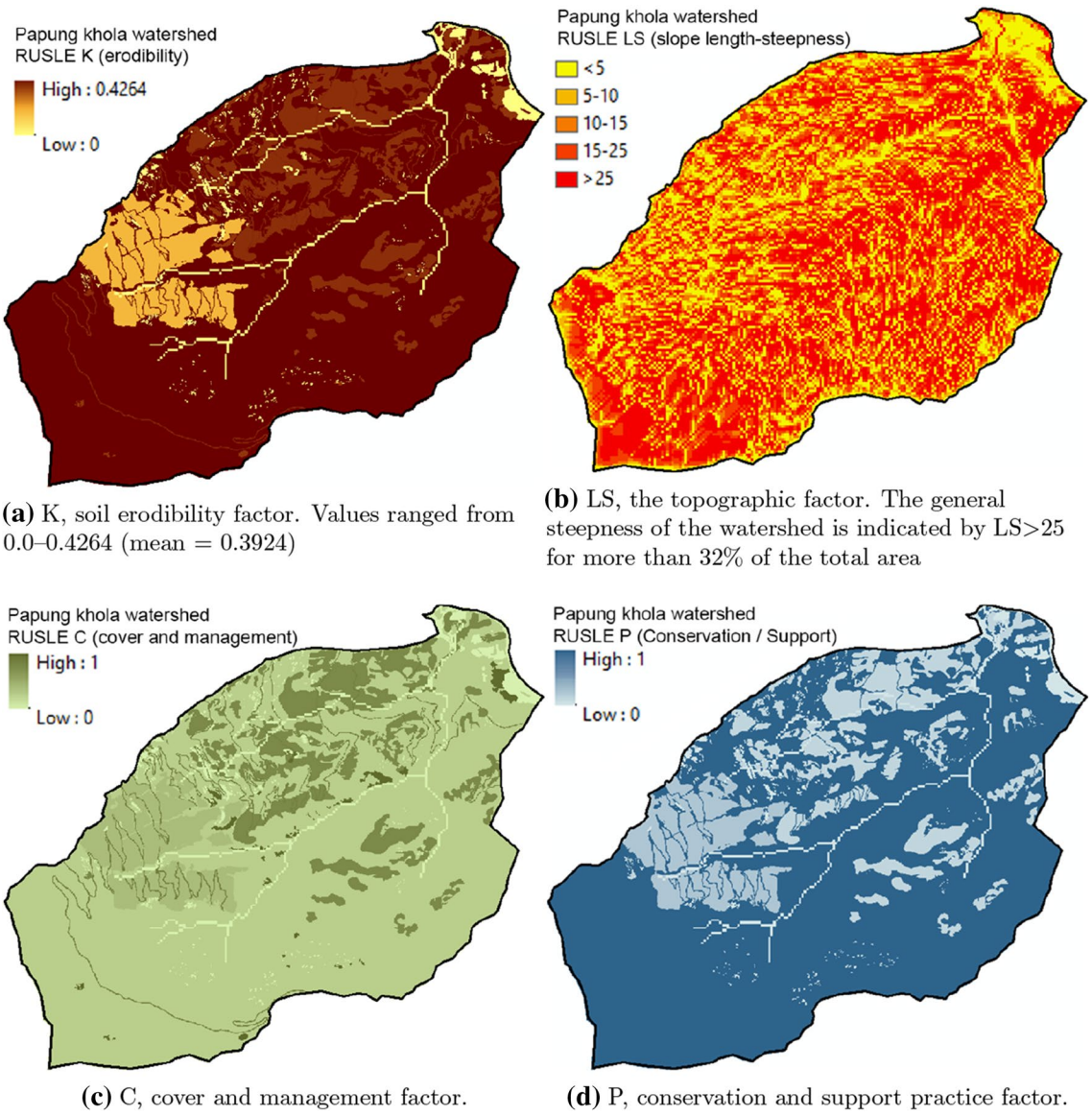

(a) K, soil erodibility factor. Values ranged from 0.0–0.4264 (mean = 0.3924)

(b) LS, the topographic factor. The general steepness of the watershed is indicated by LS>25 for more than 32% of the total area

(c) C, cover and management factor.

(d) P, conservation and support practice factor.

Fig. 4 Spatial distribution of RUSLE factors

Table 5 RUSLE soil erodibility factor (*K*) for different landuse and soil textural classes in the Papung *khola* watershed (per Das et al. 2014)

Land use class	Texture class	OM (% w/w)	*K* (erodibility)
Forest	Fine silty loam	5.53	0.4264
Multi-crop	Coarse medium loam	2.17	0.3919
Plantation	Fine sandy clay loam	5.08	0.2713
Barren	Fine sandy loam	1.47	0.3876
Roads	(* unpaved only)	–	0.40
		Mean	0.3924

Table 6 RUSLE cover and management (*C*) and conservation support practice (*P*) factors for different land-use classes (per Das et al. 2014)

Land use class	*C* factor	*P* factor
Forest	0.10	1.00
Multi-crop	0.32	0.10
Plantation	0.15	0.20
Barren	1.00	1.00
Roads	0.35	1.00
Mean	0.138	0.795

Table 7 Erosion classes by predicted coverage in the Papung *khola* catchment (ranges of Indian soil erosion classes as per Bhattacharyya et al. 2015)

Erosion class	Range (t ha^{-1})	Area (ha)	Coverage (%)
Very low	0.0–5.0	1984.15	99.74
	0.0–0.5	1476.59	74.22
	0.5–1.5	417.43	20.98
	1.5–3.0	76.46	3.84
	3.0–5.0	13.67	0.69
Low	5.0–10.0	4.27	0.21
Moderate	10.0–20.0	0.04	0.18
Severe	20.0–40.0	0.17	0.01
Very severe	> 40.0	Nil	Nil
Total	0.0–37.55	1989.35	100.00
Mean	3.53		

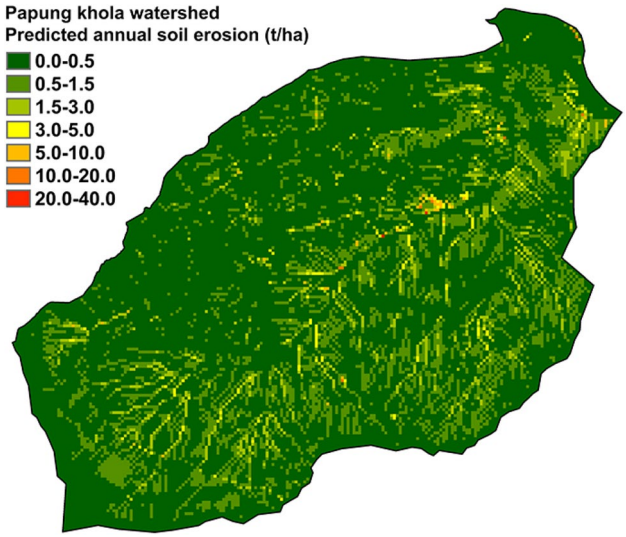

Fig. 5 Predicted, annual erosion (A) map in the Papung *khola* watershed using RUSLE. Erosion sub-classes under the major class categorized as "very low" (0.0–5.0 tons ha $^{-1}$) is shown, to clarify the spatial distribution of predicted soil erosion values at the grid cell (900 m^2) level

to prevent diversion of use will contribute to prevention of land degradation.

The above work was conducted as a preliminary study to understand the potential soil losses from a small. mixed land-use watershed, with a moderate to high slope terrain under a high precipitation regime. The modeling efforts also highlight the potential for more intense monitoring of soil quality and measurement of parameters for understanding the dynamics of soil erosion, sub-surface infiltration and overland flow, and soil moisture levels. It also illustrates the aggravation of top soil loss under high precipitation conditions under steep slopes when land use changes occur leading to removal or lowering of quality of vegetation cover.

References

Arnoldus HMJ (1980) An approximation of the rainfall factor in the Universal Soil Loss Equation. In: de Boodt M, Gabriels D (eds) Assessment of erosion. Wiley, New York, pp 127–132

Beck HE, Zimmermann NE, McVicar TR, Vergopolan N, Berg A, Wood EF (2018) Present and future Köppen–Geiger climate classification maps at 1-km resolution. Sci Data 5:180214. https://doi.org/10.1038/sdata.2018.214

Berndt C, Haberlandt U (2018) Spatial interpolation of climate variables in northern Germany–influence of temporal resolution and network density. J Hydrol Reg Stud 15:184–202. https://doi.org/10.1016/j.ejrh.2018.02.002

Bhattacharyya R, Ghosh BN, Mishra PK, Mandal B, Rao CS, Sarkar D, Das K, Anil KS, Lalitha M, Hati KM, Franzluebbers AJ (2015) Soil degradation in India: challenges and potential solutions. Sustainability 7(4):3528–3570

Compo GP, Whitaker JS, Sardeshmukh PD, Matsui N, Allan RJ, Yin X, Gleason BE, Vose RS, Rutledge G, Bessemoulin P (2011) The twentieth century reanalysis project. Q J R Meteorol Soc 137(654):1–28. https://doi.org/10.1002/qj.776

Dabral P, Baithuri N, Pandey A (2008) Soil erosion assessment in a hilly catchment of North Eastern India using USLE, GIS and remote sensing. Water Resour Manag 22(12):1783–1798. https://doi.org/10.1007/s11269-008-9253-9

Das TH, Dutta D, Reddy GPO, Singh SK, Sarkar D, Dhyani BL, Mishra PK (2014) Soil erosion: Sikkim (Technical Report). India: National Bureau of Soil Survey & Land Use Planning, Central Soil and Water Conservation Research and Training Institute. (Technical Bulletin, NBSS Publication 164)

Das TH, Sarkar D, Gajbhiye KS (2003) Soil series of Sikkim (Technical Report No. NBSS Publications 105). Nagpur, MH, 440033 India: National Bureau of Soil Survey and Land Use Planning, Indian Council of Agricultural Research

Directorate of Census Operations (2012) District Census Handbook: North, West, South And East districts (Vols. Census of India: Sikkim, Series 12, Part XII-B: Village and Town wise Primary Census Abstract (PCA)). http://www.sikenvis.nic.in/writereaddata/web-SikkimCensus2011Data.pdf. Accessed 6 Nov 2018

Fick SE, Hijmans RJ (2017) WorldClim 2: new 1-km spatial resolution climate surfaces for global land areas. Int J Climatol 37(12):4302–4315. https://doi.org/10.1002/joc.5086

Friedman D, Hubbs M, Tugel A, Seybold C, Sucik M (2001) Guidelines for soil quality assessment in conservation planning. In: Joubert B (ed) NRCS SQI, Washington DC

India Meteorological Department (2015) State-wise rainfall data for 2014 – Sikkim. http://hydro.imd.gov.in/hydrometweb/---SessionID---/Rainfallmaps.aspx, for Real-time updated past rainfall map of 2014

Ismail J, Ravichandran S (2008) RUSLE2 model application for soil erosion assessment using remote sensing and GIS. Water Resour Manag 22(1):83–102. https://doi.org/10.1007/s11269-006-9145-9

Kumar M, Krishnaswamy J (2016) Soil and rainfall monitoring in a montane watershed within the Fambong Lho Wildlife Sanctuary in the Sikkim Himalayas (2011-). (personal communication)

Laflen JM, Elliot W, Flanagan D, Meyer C, Nearing M (1997) WEPP-predicting water erosion using a process-based model. J Soil Water Conserv 52(2):96–102

Laflen JM, Elliot WJ, Simanton JR, Holzhey CS, Kohl KD (1991) WEPP: soil erodibility experiments for rangeland and cropland soils. J Soil Water Conserv 46(1):39–44

Laflen JM, Lane LJ, Foster GR (1991) WEPP: a new generation of erosion prediction technology. J Soil Water Conserv 46(1):34–38

Maharana I, Rai SC, Sharma E (2000) Environmental economics of the Khangchendzonga National Park in the Sikkim Himalaya, India. GeoJournal 50(4):329–337

Marchese C (2015) Biodiversity hotspots: a shortcut for a more complicated concept. Glob Ecol Conserv 3:297–309. https://doi.org/10.1016/j.gecco.2014.12.008

Matsuura K, Willmott CJ (2018) Terrestrial precipitation: 1900–2017 gridded monthly time series. Electronic. Department of Geography, University of Delaware, Newark, DE 19716 USA. (Archive (Version 5.01) released in August, 2018)

Mitasova H, Hofierka J, Zlocha M, Iverson LR (1996) Modelling topographic potential for erosion and deposition using GIS. Int J Geogr Inf Syst 10(5):629–641. https://doi.org/10.1080/02693799608902101

Moore ID, Burch GJ (1986) Modelling erosion and deposition: topographic effects. Trans ASAE 29(6):1624–1630. https://doi.org/10.13031/2013.30363

Moore ID, Gessler PE, Nielsen GA, Peterson GA (1993) Soil attribute prediction using terrain analysis. Soil Sci Soc Am J 57(2):443–452. https://doi.org/10.2136/sssaj1993.03615995005700020026x

Moore ID, Wilson JP (1992) Length-slope factors for the revised universal soil loss equation: simplified method of estimation. J Soil Water Conserv 47(5):423–428

Morgan R, Morgan D, Finney H (1984) A predictive model for the assessment of soil erosion risk. J Agric Eng Res 30:245–253. https://doi.org/10.1016/s0021-8634(84)80025-6

Morgan RPC, Quinton JN, Smith RE, Govers G, Poesen JWA, Auerswald K, Chisci G, Torri D, Styczen ME (1998) The European Soil Erosion Model (EUROSEM): a dynamic approach for predicting sediment transport from fields and small catchments. Earth Surface Process Landf J Br Geomorphol Group 23(6):527–544. https://doi.org/10.1002/(sici)1096-9837(199806)23:6<527::aid-esp868>3.0.co;2-5

Myers N (1990) The biodiversity challenge: expanded hot-spots analysis. The Environmentalist 10(4):243–256. https://doi.org/10.1007/bf02239720

Nearing MA, Deer-Ascough L, Laflen JM (1990) Sensitivity analysis of the WEPP hillslope profile erosion model. Trans ASAE 33(3):839–0849. https://doi.org/10.13031/2013.31409

Oliveira AH, de Freitas DAF, Neto GK, Silva MLN, da Silva MA, Curi N (2013) Development of topographic factor modeling for application in soil erosion models. INTECH Open Access Publisher. https://doi.org/10.5772/54439

Rai SC, Sharma E, Sundriyal RC (1994) Conservation in the Sikkim Himalaya: traditional knowledge and land-use of the Mamlay watershed. Environ Conserv 21(01):30–34. https://doi.org/10.1017/s0376892900024048

Rai SC, Sundriyal RC (1997) Tourism and biodiversity conservation: the Sikkim Himalaya. Ambio 26(4):235–242

Renard KG, Foster G, Weesies G, McCool D, Yoder D (1997) Predicting soil erosion by water: a guide to conservation planning with the revised universal soil loss equation (RUSLE), vol 703. United States Department of Agriculture, Washington

Rose CW, Williams JR, Sander GC, Barry DA (1983) A mathematical model of soil erosion and deposition processes: I. Theory for a plane land element. Soil Sci Soc Am J 47(5):991–995. https://doi.org/10.2136/sssaj1983.03615995004700050030x

Samanta S, Pal DK, Lohar D, Pal B (2012) Interpolation of climate variables and temperature modeling. Theor Appl Climatol 107(1):35–45. https://doi.org/10.1007/s00704-011-0455-3

Somodi I, Molnár Z, Czúcz B, Bede-Fazekas A, Bölöni J, Pásztor L, Laborczi A, Zimmermann NE (2017) Implementation and application of multiple potential natural vegetation models–a case study of Hungary. J Veg Sci 28(6):1260–1269. https://doi.org/10.1111/jvs.12564

Williams JR, Renard KG, Dyke PT (1983) Epic: a new method for assessing erosion's effect on soil productivity. J Soil Water Conserv 385:381–383

Wischmeier WH, Smith DD (1978) Predicting rainfall erosion losses—a guide to conservation planning. (Technical Report). Hyattsville, Maryland, USA: USDA. (Handbook No. 537)

Young RA, Onstad CA, Bosch DD, Anderson WP (1989) AGNPS: a nonpoint-source pollution model for evaluating agricultural watersheds. J Soil Water Conserv 44(2):168–173